

Phase diagram of the frustrated Hubbard model

R. Zitzler, N. Tong, Th. Pruschke, and R. Bulla

Center for electronic correlations and magnetism, Theoretical Physics III,
Institute of Physics, University of Augsburg, 86135 Augsburg, Germany

The Mott-Hubbard metal-insulator transition in the paramagnetic phase of the one-band Hubbard model has long been used to describe similar features in real materials like V_2O_3 . Here we show that this transition is hidden inside a rather robust antiferromagnetic insulator even in the presence of comparatively strong magnetic frustration. This result raises the question of the relevance of the Mott-Hubbard metal-insulator transition for the generic phase diagram of the one-band Hubbard model.

The microscopic description of magnetism and metal-insulator transitions constitutes one of the major research activities in modern solid state theory. Especially transition metal compounds like V_2O_3 , $LaTiO_3$, $NiS_{2-x}Se_x$ and the cuprates show metal-insulator transitions and magnetic order depending on composition, pressure or other control parameters [1]. The paramagnetic insulating phase observed in these materials is believed to be a so-called Mott-Hubbard insulator due to electron-electron correlations; in contrast to Slater or band insulators like $SrTiO_3$.

The simplest model showing both magnetism and a correlation-induced metal-insulator transition (MIT) is the one-band Hubbard model [2]

$$H = \sum_{i,j} t_{ij} c_i^\dagger c_j + \frac{U}{2} \sum_i n_i \downarrow n_i \uparrow : \quad (1)$$

Considerable progress in understanding the physics of this simple but nevertheless non-trivial model has been achieved in the last decade through the development of the dynamical mean-field theory (DMFT) [3, 4, 5]. In particular, the phase diagram for the unfrustrated Hubbard model is very well understood [4, 5]. At half-filling the physics is dominated by an antiferromagnetic insulating phase (AFI) for all $U > 0$ with a maximum $T_N \approx 0.15W$ around $U \approx W$, where W is the bandwidth of the non-interacting system. For finite doping, the antiferromagnetic phase persists up to a critical doping x_c [6] and in addition shows phase separation [7, 8]. For very large values of U the antiferromagnetic phase is replaced by a small region of Nagaoka type ferromagnetism [9, 10, 11].

Under rather special assumptions [12], it is possible to introduce complete magnetic frustration and suppress the antiferromagnetic phase. In this case, a transition from a paramagnetic metal (PM) to a paramagnetic insulator (PI) becomes visible at half-filling. At $T = 0$ it occurs at a value of the Coulomb parameter $U_c \approx 1.5W$ [5, 6, 13]. Interestingly, the transition is of first order [5, 14] for $T > 0$ with a second order end point at $T_c \approx 0.17W$ and $U_c \approx 1.2W$. Note that $T_c \approx T_N^{\max}$.

A closer look at the phase diagram of V_2O_3 [15] reveals a strikingly similar scenario, and indeed the DMFT

results for the Hubbard model have been used as a qualitative explanation [5, 16]. For a proper description of this material, however, the antiferromagnetic phase below $T_N \approx 160K$ [15] has to be taken into account. It was argued and generally accepted [5] that the introduction of partial magnetic frustration will lead to the anticipated situation, where the MIT extends beyond the antiferromagnetic phase at low temperatures. The merging of these two transitions presents an interesting problem on its own, because it is commonly believed that the magnetic transition should be of second order. Furthermore, previous results for a system with magnetic frustration show, in addition to the desired effect of reducing T_N , an extended antiferromagnetic metallic (AFM) phase at small U , preceding the transition to the AFI [5, 17]. This observation suggests an appealing possibility to link the MIT in the paramagnetic phase with a transition from an AFM to an AFI.

In this paper, we present results from a calculation using Wilson's numerical renormalization group approach (NRG) [18] and exact diagonalization techniques (ED) [20] to solve the DMFT equations [5, 19] for the Hubbard model with magnetic frustration at half-filling. We show that frustration of the magnetic interactions through incorporation of suitable long-range hopping does not lead to the previously reported sequence PM \rightarrow AFM \rightarrow AFI with an extended region of an AFM at $T = 0$ [5, 17]. Instead, we observe a first-order transition PM \rightarrow AFI. Furthermore, the reduction of T_N is too small to result in the qualitative phase diagram of V_2O_3 .

The natural choice for studying the effect of magnetic frustration is the simple hypercubic lattice with nearest and next-nearest neighbor hopping. In the DMFT, the lattice structure only enters via the dispersion of the non-interacting band states, and the corresponding k sums can conveniently be transformed into energy integrals using the free density of states (DOS) [5]. A further simplification arises if one considers lattices in the limit of large coordination number. Especially for the simple hypercubic lattice the DOS then becomes a Gaussian [3, 12] and the integrals can be performed analytically [4].

The investigation of magnetic properties is straightforward, too. In the case of the Neel state, the lattice is

divided into A and B sublattices which results in a matrix structure of the DMFT equations [5]. An antiferromagnetic Neel order then corresponds to a finite staggered magnetization $m_S > 0$ with $m_A = m_S$ and $m_B = -m_S$. Unfortunately, the Gaussian DOS of the hypercubic lattice has no real band edges, but stretches to infinity; the resulting exponential tails therefore prevent a clear distinction between metal and insulator at $T = 0$, as has been observed in a Hartree calculation for the hypercubic lattice with next-nearest neighbor hopping [21].

Georges et al. [5] suggested an extension of the DMFT equations for the Bethe lattice which introduces magnetic frustration with the DOS having finite support; this results in an analytically tractable form of the DMFT equations even for the AB-lattice.

For the standard Bethe lattice with nearest-neighbor hopping t and in the limit of infinite coordination number the DMFT equations on an AB-lattice acquire the form [5]

$$\begin{aligned} G_A(z) &= \frac{1}{z + \frac{t^2}{4} G_B(z)} ; \\ G_B(z) &= \frac{1}{z + \frac{t^2}{4} G_A(z)} ; \end{aligned} \quad (2)$$

Frustration is then introduced via additional terms in the denominators of (2) [5, 17]

$$\begin{aligned} G_A(z) &= \frac{1}{z + \frac{t^2}{4} G_B(z) + \frac{t^2}{4} G_A(z)} ; \\ G_B(z) &= \frac{1}{z + \frac{t^2}{4} G_A(z) + \frac{t^2}{4} G_B(z)} ; \end{aligned} \quad (3)$$

and the constraint $t^2 = t_1^2 + t_2^2$. In the paramagnetic case, the equations (3) reduce to those of a standard Bethe lattice which, for example, result in the well-studied Mott-transition. Furthermore, despite the frustration introduced, the system is still particle-hole symmetric. Especially for half filling this feature reduces the numerical effort quite drastically. Note that a similar suggestion exists for the hypercubic lattice [12], too.

Invoking the symmetry $G_A(z) = G_B(z)$ valid for the Neel state, eqs. (3) reduce to two coupled nonlinear equations which we solve iteratively. In the course of the iterations, the quantity $G(z)$ has to be calculated from the solution of a generalized single impurity Anderson model [5]. For that task we employ the NRG [18], suitably extended to treat spin-polarized situations [8, 22].

Let us first discuss the results for the magnetization as function of U for $T = 0$. In the following, we fix $t_2/t_1 = 1/\sqrt{3} \approx 0.58$ [23] and use the bandwidth W of the non-interacting system as our energy scale. The NRG results in Fig. 1 (circles) show a completely different behavior as compared to the ED data (diamonds) from ref. 17. Instead of a continuous increase of the stag-

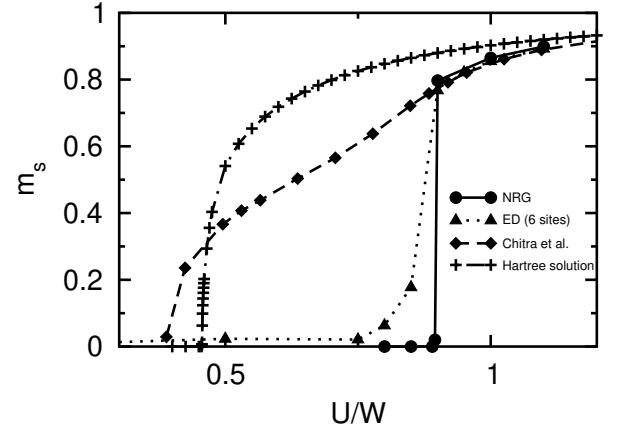


FIG. 1: Staggered magnetization m_S as function of U at $T = 0$. The circles are the results from NRG; the triangles from an ED calculation for 6 sites, while the diamonds are taken from ref. 17. For comparison, the results of a Hartree calculation are given by the crosses.

gered magnetization m_S for $U > U_c \approx 0.4W$ as suggested by both a Hartree calculation (crosses) and the data from ref. 17, we find a jump in m_S at a considerably larger $U_c \approx 0.9W$. To clarify this discrepancy, we performed ED calculations, resulting in the triangles shown in Fig. 1. We find good agreement with our NRG results, the transition systematically approaching the NRG curve with increasing size of the system diagonalized in the ED procedure. We furthermore observed a rather strong dependence of the ED results on details of the numerical procedure, especially on the energy cutoff introduced in calculating $G(z)$. Decreasing this cutoff systematically shifts the ED result towards the one found in [17]. The NRG, on the other hand, is stable with respect to changes in the parameters controlling its numerical accuracy.

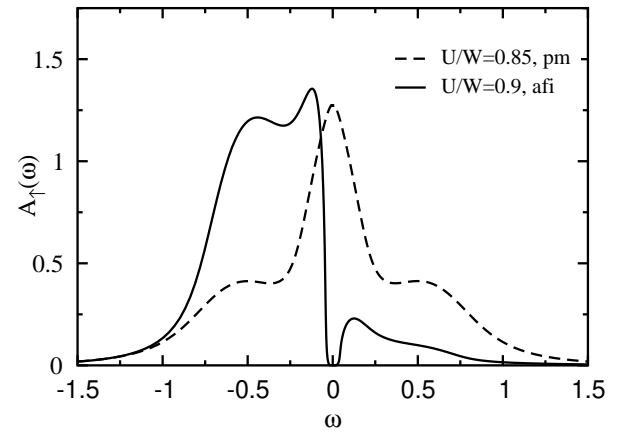


FIG. 2: Density of states for spin up on an A lattice site as function of frequency.

Another important question is the existence of an anti-

ferromagnetic metallic solution of the DMFT equations. Figure 2 shows the NRG results for the DOS for $T = 0$ and spin up on an A lattice site. Due to particle-hole symmetry the DOS for spin down on A sites (or spin up on B sites) can be obtained by $!!$. The full and dashed lines represent the AFI solution for $U < U_c$ and the PM solution for $U > U_c$, respectively. Clearly, the magnetic solution is insulating with a well-developed gap at the Fermi energy. Quite generally, we were not able to find a stable AFM solution at $T = 0$.

The discontinuity in the staggered magnetization m_s at the transition PM \leftrightarrow AFI implies a first order transition and the existence of a hysteresis region. Indeed, starting

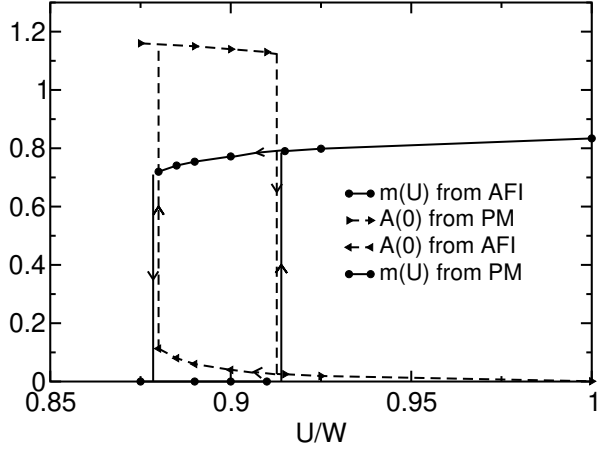


FIG. 3: Staggered magnetization (solid lines) and total DOS at the Fermi energy (dashed lines) as function of U in the vicinity of U_c for $T = 0.0155W$. The arrows indicate that the DMFT solutions have been obtained by either increasing U (\rightarrow) or decreasing U (\leftarrow).

from the paramagnet at $U = U_c$ and increasing U results in a magnetization curve different from the one obtained by starting at $U = U_c$ and decreasing U . This is apparent from Fig. 3 (full lines) where a region of hysteresis can be observed in the staggered magnetization (for temperature $T = 0.0155W$). At the same time the total DOS at the Fermi energy $A(0) = A_+(0) + A_-(0)$ shows hysteresis between metallic and insulating behavior in exactly the same U region. Note, that due to the finite temperature the DOS at the Fermi level is not exactly zero in the Neel state, but strongly reduced as compared to the metal [14].

It is of course important to verify that the hysteresis found for small U is not some kind of artefact. This can most conveniently be shown by looking at the transition at large U . Due to the mapping of the Hubbard model to a Heisenberg model in this regime, one should expect the transition to be of second order, with the staggered magnetization vanishing continuously like $m_s \propto \sqrt{T_N - T}$ when approaching T_N from below. That this is indeed the case is apparent from Fig. 4, where we show the

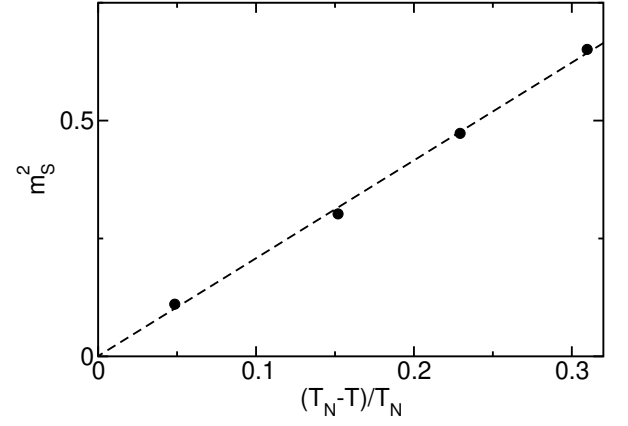


FIG. 4: Squared staggered magnetization m_s as function of T at $U=W = 2$. Note that m_s^2 vanishes continuously like $T_N - T$ as $T \rightarrow T_N$.

squared staggered magnetization as function of T for $U=W = 2$. The transition is thus of second order with the expected mean-field exponent in this region of the phase diagram.

Collecting the results for the transitions and the hysteresis region for different temperatures leads to the phase diagram in Fig. 5. An enlarged view of the re-

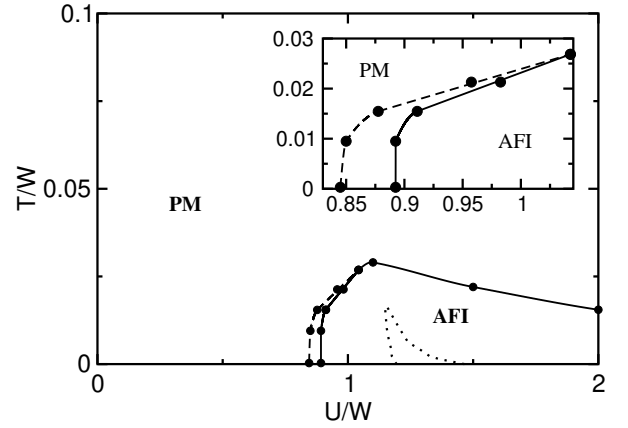


FIG. 5: Magnetic phase diagram for the Hubbard model with frustration as defined by eqs. (3) and $t_2=t_1 = 1/3$. The dotted lines inside the AFI denote the coexistence region for the paramagnetic MIT. The inset shows an enlarged view of the region with coexistence of PM and AFI.

gion showing coexistence of PM and AFI is given in the inset, where the full line represents the transition PM \rightarrow AFI with increasing U and the dashed line the transition AFI \rightarrow PM with decreasing U . These two lines seem to merge at a value of $U = W$ for this particular value of t_2 , with a critical temperature for this endpoint $T_c = 0.02W$. Note that, even in the presence of such a sizeable t_2 , the antiferromagnetic phase still completely

encompasses the paramagnetic Mott (dotted lines in the main panel of Fig. 5 [14]).

It is, of course, interesting to see how the magnetic phase evolves with increasing t_2 and in particular how its boundary crosses the paramagnetic Mott. We find that increasing t_2 does not change the form of the magnetic phase in Fig. 5 qualitatively, but mainly shifts the lower

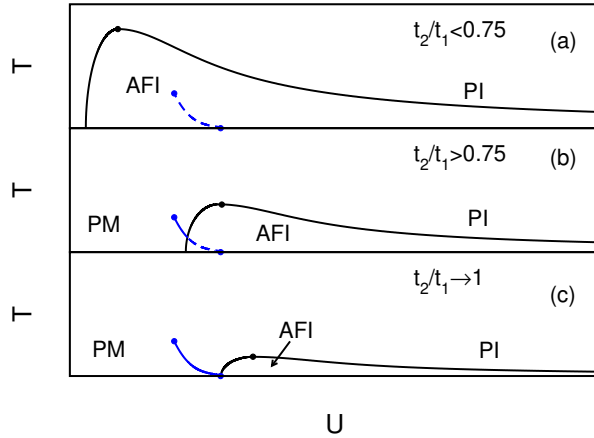


FIG. 6: Schematic evolution of the magnetic phase diagram with increasing frustration. The dots on the phase transition lines denote the critical endpoints of the first order transitions.

critical U and decreases the maximum T_N . The calculated estimates for those two quantities as function of t_2 lead to the schematic evolution of the phase diagram presented in Fig. 6a-c. Here, only the true phase boundaries are shown. A direct calculation of the free energy at finite temperatures is presently not possible with the NRG method, so we cannot calculate the actual transition line separating the paramagnetic and AF phases. The transition lines in Fig. 6a-c are therefore a guide to the eye only. For the Mott transition, the position of the actual transition line has been calculated in ref. 24.

Figure 6a shows the qualitative phase diagram corresponding to Fig. 5 with the line of first order transitions ending in a critical point. Upon further increasing the value of t_2 , the first order transition lines from both the PM \leftrightarrow AFI and the Mott transition cross (Fig. 6b), thus exposing a finite region of the Mott insulator and a transition PM \leftrightarrow AFI. Finally, for even higher values of t_2 , the PM \leftrightarrow AFI transition at $T = 0$ approaches the Mott transition and T_N is reduced significantly (Fig. 6c). Note that in the limiting case $t_2 = t_1$ the AFI phase completely vanishes due to the structure of the DMFT equations (3). However, for $t_2 \neq t_1$ there is always a finite antiferromagnetic exchange $J / (t_1^2 - t_2^2) = U$ which is sufficient to stabilize an antiferromagnetic ground state for $U > U_c$ of the Mott transition.

From these results we conclude that frustration as introduced via eqs. (3) is not sufficient to qualitatively reproduce the phase diagram of materials like V_2O_3 . In

particular, the Mott transition extends beyond the AFI region only for unphysically large values of t_2 .

The question remains whether it is possible at all to reproduce qualitatively the scenario observed in V_2O_3 within a one-band model. Based on our results reported here, we rather believe that one has to take into account additional degrees of freedom, for example phonons (within a Holstein-Hubbard model) or orbital degeneracies (within a multiband Hubbard model).

We acknowledge useful conversations with M. Vojta, G. Kotliar, R. Chitra and P. J. G. van Dongen. This work was supported by the DFG through the collaborative research center SFB 484, the Leibniz Computer center and the Computer center of the Max-Planck-Gesellschaft in Garching. NT acknowledges the support by the Alexander von Humboldt foundation.

-
- [1] M. Imada, A. Fujimori, and Y. Tokura, Rev. Mod. Phys. 70, 1039 (1998).
 - [2] J. Hubbard, Proc. R. Soc. London A 276, 238 (1963); M. C. Gutzwiller, Phys. Rev. Lett. 10, 59 (1963); J. Kanamori, Prog. Theor. Phys. 30, 275 (1963).
 - [3] W. Metzner und D. Vollhardt, Phys. Rev. Lett. 62, 324 (1989).
 - [4] T. Puschke, M. Jarrell and J. K. Freericks, Adv. Phys. 42, 187 (1995);
 - [5] A. Georges, G. Kotliar, W. Krauth and M. J. Rozenberg, Rev. Mod. Phys. 68, 13 (1996).
 - [6] M. Jarrell and Th. Puschke, Z. Phys. B 90, 187 (1993).
 - [7] P. J. G. van Dongen, Phys. Rev. Lett. 67, 757 (1991); Phys. Rev. B 50, 14016 (1994).
 - [8] R. Zitzler, Th. Puschke, R. Bulla, Eur. Phys. J. B 27, 473 (2002).
 - [9] Y. Nagaoka, Phys. Rev. 147, 392 (1966).
 - [10] Th. Oebmeyer, Th. Puschke and J. Keller, Phys. Rev. B 56, R 8479 (1997).
 - [11] D. Vollhardt, N. Blümer, K. Held, M. Köllar, J. Schlipf and M. Ullrich, Z. Phys. B 103, 283 (1997); M. Ullrich, Eur. Phys. J. B 1, 301 (1998).
 - [12] E. Müller-Hartmann, Z. Phys. B 76, 211 (1989).
 - [13] R. Bulla, Phys. Rev. Lett. 83, 136 (1999).
 - [14] R. Bulla, T. A. Costi, D. Vollhardt Phys. Rev. B 64, 045103 (2001).
 - [15] D. B. McWhan, and J. P. Remeika, Phys. Rev. B 2, 3734 (1970); D. B. McWhan et al., Phys. Rev. B 7, 1920 (1973).
 - [16] M. J. Rozenberg et al., Phys. Rev. Lett. 75, 105 (1995).
 - [17] R. Chitra, G. Kotliar, Phys. Rev. Lett. 83, 2386 (1999).
 - [18] K. G. Wilson, Rev. Mod. Phys. 47, 773 (1975); H. R. Krishna-murthy, J. W. Wilkins, and K. G. Wilson, Phys. Rev. B 21, 1003 (1980); ibid. 21, 1044 (1980).
 - [19] R. Bulla, A. C. Hewson and Th. Puschke, J. Phys. { Condens. Matter 10, 8365 (1998).
 - [20] M. Caarel and W. Krauth, Phys. Rev. Lett. 72, 1545 (1994).
 - [21] W. Hofstetter, D. Vollhardt, Ann. Physik 7, 48 (1998).
 - [22] T. A. Costi, Phys. Rev. Lett. 85, 1504 (2000); W. Hofstetter, Phys. Rev. Lett. 85, 1508 (2000).
 - [23] This value is the same as the one used in [5, 17]

- [24] N.H. Tong, S.Q. Shen and F.C. Pu, Phys. Rev. B 64, 235109 (2001).